Stable Path Tracking With JEMRMS Through Vibration Suppression Algorithmic Singularities Using Momentum Conservation

N. Hara*, Y. Kanamiya** and D. Sato**

Department of Mechanical Systems Engineering, Graduate School of Engineering,
Tokyo City University, Japan
*e-mail: hara@rls.mse.tcu.ac.jp, **e-mail: {nenchev, dsato}@tcu.ac.jp

Abstract

A new path tracking control method for the Japanese Experiment Module Remote Manipulator System (JEMRMS) / Small Fine Arm (SFA) "macro-mini" manipulator system on the International Space Station is proposed. The method ensures *almost* reactionless motion within wide areas of workspace. This feature is achieved via continuous inertial damping of the vibrations in the first three joints of the macro part (JEMRMS), using vibration suppression control with the nine-DOF mini-arm (SFA plus the last three joints of JEMRMS). To deal with persisting algorithmic singularities due to the constraints imposed via the path tracking and vibration suppression subtasks, we propose to use reactionless motion instead of vibration suppression while crossing the algorithmic singularity. Such motion is ensured by conserving the inertia coupling momentum upon entering a suitably defined neighborhood of the singularity. In contrast to previous studies, where momentum has been conserved at zero, here the momentum is conserved at a nonzero value. This helps avoiding other types of algorithmic singularities which are due to the reactionless motion control subtask.

The performance of the method is examined via simulations. Results from two other methods, known from previous studies, are obtained and compared with those from the proposed method. These results clearly demonstrate that stable control can be achieved while passing through algorithmic singularities.

1 Introduction

Dexterous tasks, in space, have still to be completed manually during extra-vehicular activities of an astronaut attached to the end of a robot arm or to a safety tether. To avoid risks, it is expected that the tasks will be assigned to dexterous robots mounted on the tip of a large arm. Such robot systems, referred to as "macro-mini manipulator systems," are known from past studies [1]. One such system is JEMRMS/SFA which is composed of a large manipulator with flexible joints and a single small arm. When operating only the large manipulator, some of the well known methods for flexible-joint manipulator control [2] may be considered as an appropriate choice to suppress the residual vibrations in the joints. When operated together with the small arm (SFA), however, inertial damping may be a better alternative as discussed in [3]. The reasoning is that in such mode of operation, the role envisioned for JEMRMS is just relocation of the SFA base. This means that the joints will be locked while the SFA operates. Under such circumstances, it might be appropriate to treat JEMRMS as a flexible base and to apply respective methods for flexible-base vibration suppression control.

We must note that in previous works on JEMRMS/SFA, e.g. in [4], the flexible base was modeled as a single flexible body with six independent flexural coordinates. This representation requires an additional mapping from the flexible joint variables of the macro arm to the flexural variables concentrated at the tip of the macro arm, where the mini-arm is attached. On the other hand, in our previous work [5], JEMRMS/SFA was modeled as a hybrid system comprising both flexible passive joints (first three joints of JEMRMS) and rigid active joints (the rest of the JEMRMS plus the SFA joints). We have developed an integrated motion control method composed of control components for vibration suppression and reactionless motion. However, it became apparent that path planning for the small arm presents a significant difficulty due to the existence of so-called algorithmic singularities. In the vicinity of such singularities not only DOFs are lost, but also, the system becomes unstable. In contrast to kinematic singularities, the singularity loci of such algorithmic singularities change with the variation of the arm configuration, which renders path planning for singularity avoidance a very difficult problem.

The aim of this work is to propose a stable control method for simultaneous path tracking and vibration suppression in the presence of algorithmic singularities. Especially, we focus on achieving a sufficiently wide operational workspace via a capability for passing through algorithmic singularities. It is shown that such capability can be ensured when the mini-arm CoM velocity is constant while moving through the algorithmic singularity. This

results in reactionless motion without inducing vibrations in the flexible joints. We should note that our method is model-based, and the model treated here is assumed to be perfect. Issues related to model uncertainty and robustness will be treated in a forthcoming study.

2 Background and Notation

First, we introduce the flexible-base notation. Thereafter, we will rewrite the system equation for the treatment with passive flexible joints.

2.1 Equation of motion

The equation of motion of an n-DOF manipulator, mounted on a flexible base with k flexural coordinates (see Figure 1), has the form of an underactuated system. It can be written as follows [6]:

$$\begin{bmatrix} \boldsymbol{H}_b & \boldsymbol{H}_{bm} \\ \boldsymbol{H}_{bm}^T & \boldsymbol{H}_m \end{bmatrix} \begin{bmatrix} \dot{\mathcal{V}}_b \\ \ddot{\boldsymbol{q}} \end{bmatrix} + \begin{bmatrix} \boldsymbol{D}_b & \boldsymbol{0} \\ \boldsymbol{0} & \boldsymbol{D}_m \end{bmatrix} \begin{bmatrix} \mathcal{V}_b \\ \dot{\boldsymbol{q}} \end{bmatrix} + \begin{bmatrix} \boldsymbol{K}_b & \boldsymbol{0} \\ \boldsymbol{0} & \boldsymbol{0} \end{bmatrix} \begin{bmatrix} \Delta\boldsymbol{\xi}_b \\ \boldsymbol{q} \end{bmatrix} + \begin{bmatrix} \boldsymbol{c}_b \\ \boldsymbol{c}_m \end{bmatrix} = \begin{bmatrix} \boldsymbol{0} \\ \boldsymbol{\tau} \end{bmatrix}, \quad (1)$$

where $\Delta\boldsymbol{\xi}_b \in \Re^k$ is the spatial deflection of the flexible base from its equilibrium, $\mathcal{V}_b \in \Re^k$ is the base twist (spatial velocity), $\boldsymbol{q} \in \Re^n$ stands for the joint coordinates of the arm, $\boldsymbol{H}_b$, $\boldsymbol{D}_b$ and $\boldsymbol{K}_b \in \Re^{k\times k}$ denote base inertia, damping and stiffness, respectively. $\boldsymbol{H}_m(\boldsymbol{q}) \in \Re^{n\times n}$ is the inertia matrix of the arm. $\boldsymbol{H}_{bm}(\Delta\boldsymbol{\xi}_b, \boldsymbol{q}) \in \Re^{k\times n}$ denotes the *inertia coupling matrix*. $\boldsymbol{c}_b(\Delta\boldsymbol{\xi}_b, \mathcal{V}_b, \boldsymbol{q}, \dot{\boldsymbol{q}})$ and $\boldsymbol{c}_m(\Delta\boldsymbol{\xi}_b, \mathcal{V}_b, \boldsymbol{q}, \dot{\boldsymbol{q}})$ are velocity-dependent nonlinear terms. $\boldsymbol{D}_m$ denotes joint damping and $\boldsymbol{\tau} \in \Re^n$ is the joint torque. No external force is acting neither on the base nor on the manipulator because of assuming in space.

2.2 Dual control task formulation

Our aim is to simultaneously control the motion of both end-links: the flexible base and the end-effector. A computed torque control has been employed in previous studies [7] of the type:

$$\boldsymbol{\tau} = \boldsymbol{H}_m\ddot{\boldsymbol{q}}^{ref} + \boldsymbol{H}_{bm}^T\dot{\mathcal{V}}_b + \boldsymbol{D}_m\dot{\boldsymbol{q}} + \boldsymbol{c}_m, \quad (2)$$

where $\ddot{\boldsymbol{q}}^{ref}$ is the reference joint acceleration which can be determined in different ways, depending on the specific control subtask.

Consider first the base motion control subtask. Base motion control can be achieved via proper manipulator control, using inertial coupling [6]. The equation of motion of the base is extracted from the upper part of the equation of motion (1):

$$\boldsymbol{H}_b\dot{\mathcal{V}}_b + \boldsymbol{D}_b\mathcal{V}_b + \boldsymbol{K}_b\Delta\boldsymbol{\xi}_b = -\boldsymbol{H}_{bm}\ddot{\boldsymbol{q}} - \dot{\boldsymbol{H}}_{bm}\dot{\boldsymbol{q}}, \quad (3)$$

where the approximation $\boldsymbol{c}_b \approx \dot{\boldsymbol{H}}_{bm}\dot{\boldsymbol{q}}$ was used. The quantity on the r.h.s. is the *base reaction wrench*. It is derived

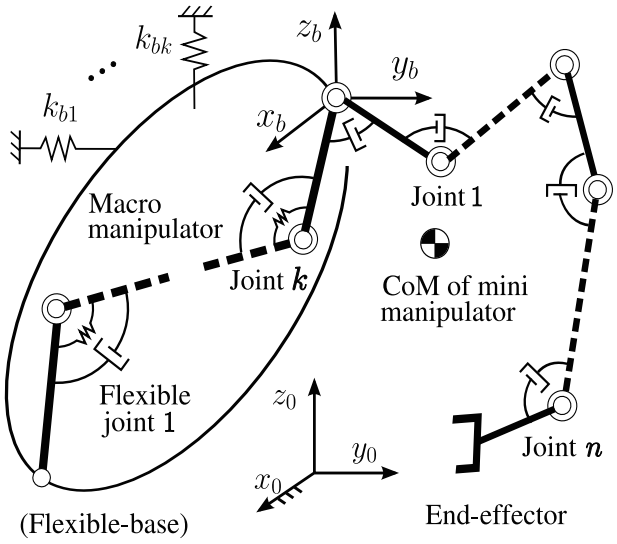

Figure 1. Flexible-base manipulator system.

via Newton's law of action and reaction from the *imposed wrench* $\mathcal{W}_m$ w.r.t. the base coordinate frame due to manipulator motion:

$$\mathcal{W}_b = -\mathcal{W}_m = -\boldsymbol{H}_{bm}\ddot{\boldsymbol{q}} - \dot{\boldsymbol{H}}_{bm}\dot{\boldsymbol{q}}. \quad (4)$$

The imposed wrench can be represented as the time derivative of the spatial momentum of the manipulator:

$$\mathcal{W}_m = \frac{d}{dt}\mathcal{L}_m = \frac{d}{dt}(\boldsymbol{H}_{bm}\dot{\boldsymbol{q}}). \quad (5)$$

$\mathcal{L}_m$ will be denoted also as the *coupling momentum*. The manipulator does not induce any reactions to the base, if the coupling momentum is conserved: $\mathcal{L}_m = \text{const.} \Leftrightarrow \mathcal{W}_m = \boldsymbol{0}$. Based on these relations, two suitable candidates have been considered as base motion control subtasks in past studies [7]: (i) reactionless motion and (ii) vibration suppression.

Reactionless motion control can be achieved with a zero imposed wrench. From (4), we have:

$$\mathcal{W}_m^{ref} = \boldsymbol{H}_{bm}\ddot{\boldsymbol{q}} + \dot{\boldsymbol{H}}_{bm}\dot{\boldsymbol{q}} = \boldsymbol{0}. \quad (6)$$

Then, the reference joint acceleration for reactionless motion can be derived as:

$$\ddot{\boldsymbol{q}}^{ref} = -\boldsymbol{H}_{bm}^{+}\dot{\boldsymbol{H}}_{bm}\dot{\boldsymbol{q}} + \boldsymbol{n}_{bm}, \quad (7)$$

where $(\circ)^+$ denotes the pseudoinverse and $\boldsymbol{n}_{bm}$ is a vector from the kernel of the inertia coupling matrix. The set of all such vectors is referred to as the *Reaction Null-Space* [7].

The vibration suppression control subtask, on the other hand, damps out induced base vibrations via the reference wrench:

$$\mathcal{W}_m^{ref} = -\mathcal{W}_b^{ref} = \boldsymbol{G}_b\mathcal{V}_b, \quad (8)$$

where $\boldsymbol{G}_b$ denotes a positive definite matrix for spatial additional (inertial) damping and ${}^{\prime}\boldsymbol{\mathcal{V}}_b$ is measured base spatial velocity. This will lead to a damped vibrational subsystem for the base:

$$\boldsymbol{H}_b {}^{\prime}\dot{\boldsymbol{\mathcal{V}}}_b + (\boldsymbol{D}_b + \boldsymbol{G}_b) {}^{\prime}\boldsymbol{\mathcal{V}}_b + \boldsymbol{K}_b \Delta\boldsymbol{\xi}_b = \boldsymbol{0}. \tag{9}$$

The reference joint acceleration for vibration suppression can be obtained as:

$$\ddot{\boldsymbol{q}}^{ref} = \boldsymbol{H}_{bm}^{+}(\boldsymbol{G}_b {}^{\prime}\boldsymbol{\mathcal{V}}_b - \dot{\boldsymbol{H}}_{bm}\dot{\boldsymbol{q}}) + \boldsymbol{n}_{bm}. \tag{10}$$

Comparing (7) and (10), it becomes apparent that actually (10) includes (7).

Next, consider the end-effector task. Denote by ${}^{\prime}\boldsymbol{\mathcal{V}}_e = [\boldsymbol{v}_e^T \;\; \boldsymbol{\omega}_e^T]^T \in \Re^6$ the end-effector spatial velocity w.r.t. the inertial coordinate frame. Its rate is:

$$ {}^{\prime}\dot{\boldsymbol{\mathcal{V}}}_e = \boldsymbol{J}_e\ddot{\boldsymbol{q}} + \dot{\boldsymbol{J}}_e\dot{\boldsymbol{q}} + {}^{\prime}\dot{\boldsymbol{\mathcal{V}}}_b, \tag{11}$$

where $\boldsymbol{J}_e(\boldsymbol{q}) \in \Re^{6\times n}$ stands for the end-effector Jacobian w.r.t. the base coordinate frame. The above equation can be easily reformulated for path tracking, by including feedback components for the spatial end-effector error and its derivative:

$$ {}^{\prime}\dot{\boldsymbol{\mathcal{V}}}_e^{ref} = {}^{\prime}\dot{\boldsymbol{\mathcal{V}}}_e^{d} + \boldsymbol{K}_d({}^{\prime}\boldsymbol{\mathcal{V}}_e^{d} - {}^{\prime}\boldsymbol{\mathcal{V}}_e) + \boldsymbol{K}_p(\boldsymbol{\xi}_e^{d} - \boldsymbol{\xi}_e), \tag{12}$$

where superscript $(\circ)^d$ denotes a desired value, $\boldsymbol{\xi}_e$ is the spatial position/orientation of the end-effector and $\boldsymbol{K}_d$ and $\boldsymbol{K}_p$ are positive definite diagonal feedback gain matrices.

The motion control subtasks for the two end-links can be combined as follows:

$$\begin{bmatrix} {}^{\prime}\dot{\boldsymbol{\mathcal{V}}}_e^{ref} \\ {}^{\prime}\boldsymbol{\mathcal{W}}_m^{ref} \end{bmatrix} = \boldsymbol{A}\ddot{\boldsymbol{q}} + \dot{\boldsymbol{A}}\dot{\boldsymbol{q}} + \begin{bmatrix} {}^{\prime}\dot{\boldsymbol{\mathcal{V}}}_b \\ \boldsymbol{0} \end{bmatrix}, \tag{13}$$

where $\boldsymbol{A} = [\boldsymbol{J}_e^T \;\; \boldsymbol{H}_{bm}^T]^T \in \Re^{(6+k)\times n}$ and ${}^{\prime}\boldsymbol{\mathcal{W}}_m^{ref}$ is obtained either from (6) or from (8). The reference joint acceleration can then be written as:

$$\ddot{\boldsymbol{q}}^{ref} = \boldsymbol{A}^{+}\left(\begin{bmatrix} {}^{\prime}\dot{\boldsymbol{\mathcal{V}}}_e^{ref} \\ {}^{\prime}\boldsymbol{\mathcal{W}}_m^{ref} \end{bmatrix} - \dot{\boldsymbol{A}}\dot{\boldsymbol{q}} - \begin{bmatrix} {}^{\prime}\dot{\boldsymbol{\mathcal{V}}}_b \\ \boldsymbol{0} \end{bmatrix}\right) + \boldsymbol{n}_A, \tag{14}$$

where $\boldsymbol{n}_A$ is a vector from the kernel of $\boldsymbol{A}$[1].

It should be clear that if a control law is based on the above joint acceleration, in the neighborhood of singularities of $\boldsymbol{A}$, where $\det(\boldsymbol{A}\boldsymbol{A}^T) = 0$, performance will inevitably degrade and the system may destabilize. These singularities include the subset of kinematic singularities defined by the condition $\det(\boldsymbol{J}_e\boldsymbol{J}_e^T) = 0$. Other singularity subsets are of dynamic nature and are located within the workspace. The loci of these singularities change continuously as a function of the manipulator configuration. We will refer to these singularities as *algorithmic singularities*. Motion planning in the presence of such singularities is considered as a very difficult or impossible task.

One simple way to deal with algorithmic singularities is to fully relax one of the control subtasks within a suitably defined neighborhood of the singularity. Usually, the end-effector subtask is considered to be of higher priority, so one would prefer to relax the subtask for the base. Such strategy is easier to implement when (14) is resolved via reduction as [8]:

$$\ddot{\boldsymbol{q}}^{ref} = \boldsymbol{J}_e^{+}\left({}^{\prime}\boldsymbol{\mathcal{V}}_e^{ref} - \dot{\boldsymbol{J}}_e\dot{\boldsymbol{q}} - {}^{\prime}\boldsymbol{\mathcal{V}}_b\right) + \boldsymbol{n}_{J_e}({}^{\prime}\boldsymbol{\mathcal{W}}_m^{ref}), \tag{15}$$

where the second term on the r.h.s. denotes the subset of vectors in the kernel of the manipulator Jacobian which are dependent upon the imposed wrench.

3 Reactionless Path Tracking Control Through Algorithmic Singularities

With the above mentioned subtask relaxation approach, one could argue that if the singularity neighborhood could be defined as sufficiently small, the base disturbance would be insignificant since it will be immediately suppressed after leaving the neighborhood [8]. Nevertheless, we think that such disturbance may be still undesirable in some cases.

The magnitude of base disturbance depends on the rate of the *coupling momentum* $\boldsymbol{\mathcal{L}}_m$. This suggests a momentum conservation strategy for minimizing base disturbance. Such a strategy can be easily achieved by inserting a zero imposed wrench in (14) and (15). Thus, upon entering a suitably defined neighborhood of the singularity, the imposed wrench term is switched from vibration suppression (${}^{\prime}\boldsymbol{\mathcal{W}}_m = \boldsymbol{G}_b {}^{\prime}\boldsymbol{\mathcal{V}}_b$) to momentum conservation (${}^{\prime}\boldsymbol{\mathcal{W}}_m = \boldsymbol{0}$). The secondary task is switched back from momentum conservation to vibration suppression after leaving the singularity. Hence, the reference imposed wrench is defined as:

$${}^{\prime}\boldsymbol{\mathcal{W}}_m^{ref} = \begin{cases} \boldsymbol{G}_m(\bar{\boldsymbol{\mathcal{L}}}_m^{d} - \boldsymbol{\mathcal{L}}_m) & \text{if } t_{in} \le t \le t_{out} \\ \boldsymbol{G}_b {}^{\prime}\boldsymbol{\mathcal{V}}_b & \text{otherwise,} \end{cases} \tag{16}$$

where t_{in} and t_{out} denote time instances for entering and leaving the singularity neighborhood, respectively, $\boldsymbol{G}_m$ denotes a positive definite matrix. The desired *constant* momentum $\bar{\boldsymbol{\mathcal{L}}}_m^{d} = \boldsymbol{\mathcal{L}}_m(t_{in})$ is determined in a "sample-and-hold" manner[2].

As already mentioned, momentum conservation has been exploited also in past studies. Thereby, zero initial conditions have been assumed and hence, the momentum was conserved at zero, ensuring thereby reactionless motion throughout the entire path. We must note that such

[1] $\boldsymbol{n}_A$ is null when there are no redundant DOFs: $6 + k = n$.

[2] Henceforth, a constant value will be denoted via an overbar.

strategy is quite restrictive in the sense that reactionless motion is possible only within a very limited subspace of the entire workspace. In contrast, here we aim at ensuring *almost* reactionless motion throughout large portions of workspace, the neighborhood of algorithmic singularities included. The above momentum conservation approach with nonzero initial conditions is quite helpful.

4 Application to JEMRMS/SFA

4.1 Model

The kinematic models with parameters for JEMRMS with SFA is shown in Figure 2. Besides the kinematic parameters, the models include joint viscous damping in all joints, and joint torsional springs in the first three joints of JEMRMS. Indeed, it was pointed out [9] that the prevailing flexibilities in JEMRMS are in the joints, rather than in the links. The rest of the structure, including the three proximal joints of JEMRMS plus the six joints of SFA, is regarded as a nine-DOF redundant mini manipulator (see Figure 3). The values of the parameters used in this study, including link lengths ($l_1 - l_{12}$), masses, inertias and positions of CoM, are the same as those reported in our previous work [5].

It must be noted that the axes z_6 (z_b) and z_7 in Figure 2 are parallel and only slightly displaced. This means that one of the DOFs of the mini-arm will influence the motion very little. Nevertheless, below we will use the faithful model, without any reduction. As already mentioned, the macro arm is represented here as a structure with three passive flexible joints, and not as a single flexible body with six independent flexural coordinates, as in [4]. Since JEMRMS has joint angle sensors both at the motor axes (resolvers) and at the output axes (optical encoders) [9], it is possible to evaluate the vibration in the joints constituting the flexible joints, as required by the proposed control law.

Referring to (1), the equation of motion for JEMRMS/SFA is written in the following form[3]:

$$\begin{bmatrix} \boldsymbol{H}_M & \boldsymbol{H}_{Mm} \\ \boldsymbol{H}_{Mm}^T & \boldsymbol{H}_m \end{bmatrix} \begin{bmatrix} \ddot{\boldsymbol{q}}_M \\ \ddot{\boldsymbol{q}}_m \end{bmatrix} + \begin{bmatrix} \boldsymbol{D}_M & \boldsymbol{0} \\ \boldsymbol{0} & \boldsymbol{D}_m \end{bmatrix} \begin{bmatrix} \dot{\boldsymbol{q}}_M \\ \dot{\boldsymbol{q}}_m \end{bmatrix} + \begin{bmatrix} \boldsymbol{K}_M & \boldsymbol{0} \\ \boldsymbol{0} & \boldsymbol{0} \end{bmatrix} \begin{bmatrix} \boldsymbol{q}_M \\ \boldsymbol{q}_m \end{bmatrix} + \begin{bmatrix} \boldsymbol{c}_M \\ \boldsymbol{c}_m \end{bmatrix} = \begin{bmatrix} \boldsymbol{0} \\ \boldsymbol{\tau} \end{bmatrix}, \quad (17)$$

where $\boldsymbol{q}_m \in \Re^9$ is the joint angle vector of the mini manipulator, $\boldsymbol{H}_m(\boldsymbol{q}_m) \in \Re^{9\times9}$ is the inertia matrix of the mini manipulator and $\boldsymbol{q}_M \in \Re^3$ is the joint angle vector of the macro manipulator, $\boldsymbol{H}_{Mm}(\boldsymbol{q}_M, \boldsymbol{q}_m) \in \Re^{3\times9}$ is the inertia coupling matrix, $\boldsymbol{H}_M(\boldsymbol{q}_M) \in \Re^{3\times3}$, $\boldsymbol{D}_M \in \Re^{3\times3}$ and $\boldsymbol{K}_M \in \Re^{3\times3}$ are inertia, damping and stiffness matrices

[3] $(\circ)_M$, $(\circ)_m$ and $(\circ)_{Mm}$ stand for terms of the macro part, the mini part, and the coupling between the macro part and mini parts, respectively.

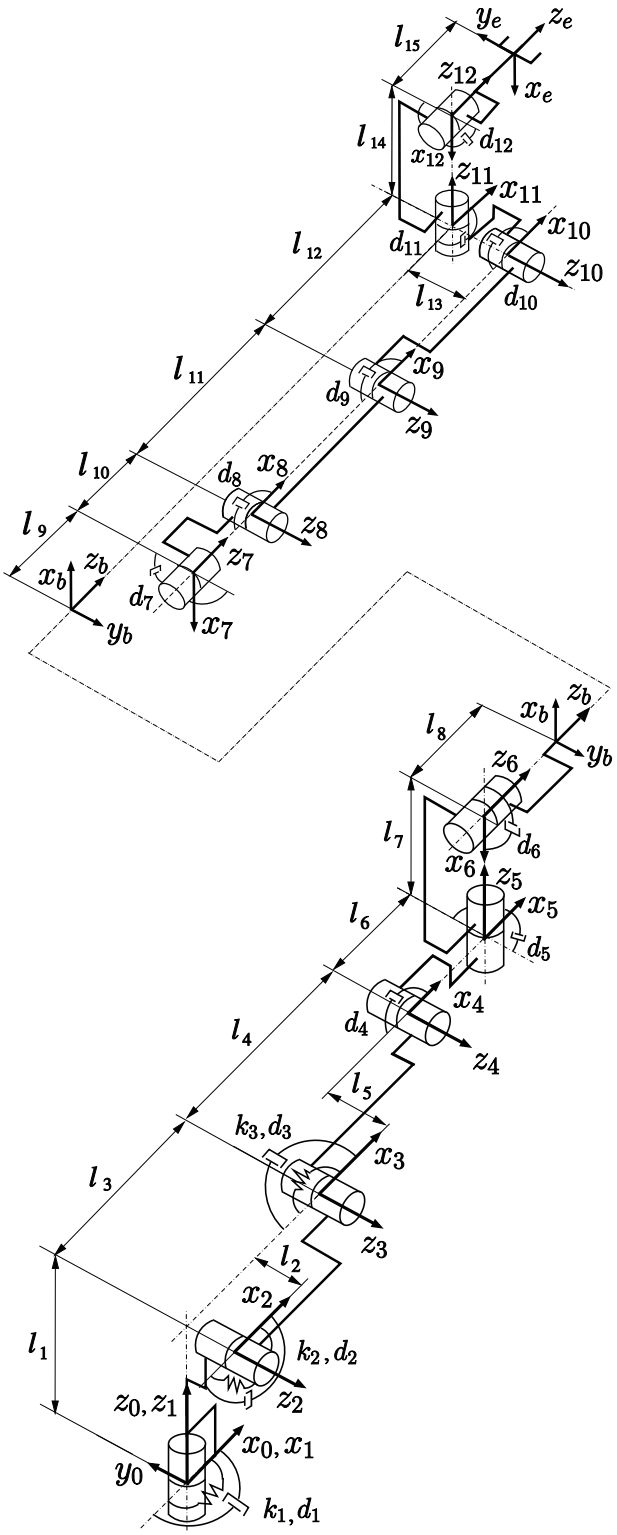

Figure 2. Kinematic structure of JEMRMS (lower figure) and SFA (upper figure).

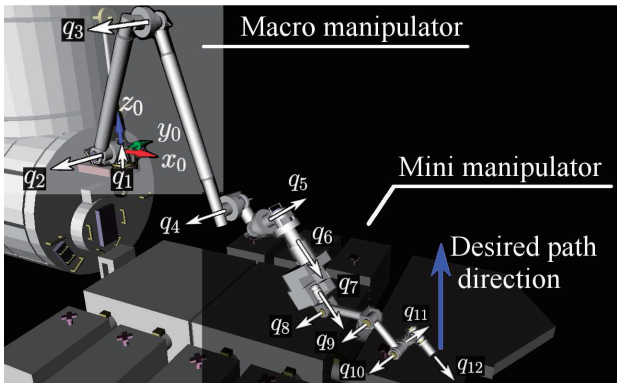

Figure 3. Macro manipulator (q_1–q_3) and mini manipulator (q_4–q_{12}). This is the initial configuration and the desired path direction used in the simulations.

of the macro manipulator. $\boldsymbol{c}_M(\boldsymbol{q}_M, \dot{\boldsymbol{q}}_M, \boldsymbol{q}_m, \dot{\boldsymbol{q}}_m) \in \Re^3$ and $\boldsymbol{c}_m(\boldsymbol{q}_M, \dot{\boldsymbol{q}}_M, \boldsymbol{q}_m, \dot{\boldsymbol{q}}_m) \in \Re^9$ denote velocity-dependent nonlinear terms, $\boldsymbol{D}_m \in \Re^{9\times9}$ stands for mini manipulator joint damping and $\boldsymbol{\tau} \in \Re^9$ is the mini manipulator joint torque vector.

4.2 Proposed control law

We consider a specific class of tasks with prevailing translational motion. This implies that the magnitude of manipulator linear momentum and its rate will be larger than that of angular momentum, and henceforth, we ignore the latter.

Further on, we consider the case when just one DOF will be lost while the mini manipulator passes through an algorithmic singularity. This means that around the singularity, the mini manipulator will be able to control only eight variables: six for the end-effector and two for the momentum. Therefore, in the equation below we ignore the momentum coordinate along x (see Figure 3). Combining the two subtasks, we obtain the control torque as follows[4]:

$$\boldsymbol{\tau}_{mcc} = \boldsymbol{H}_m \boldsymbol{A}_{\tilde{x}}^{+} \left(\begin{bmatrix} \dot{\boldsymbol{V}}_e^{ref} \\ \dot{\boldsymbol{W}}_m^{ref} \end{bmatrix} - \dot{\boldsymbol{A}}_{\tilde{x}} \dot{\boldsymbol{q}} \right) + \boldsymbol{H}_m \boldsymbol{n}_{\boldsymbol{A}_{\tilde{x}}} + (\boldsymbol{D}_m + \boldsymbol{D}_{mc}) \dot{\boldsymbol{q}}_m + \boldsymbol{c}_m, \quad (18)$$

where

$$\boldsymbol{A}_{\tilde{x}} = \begin{bmatrix} \boldsymbol{J}_m \\ \boldsymbol{H}_{bm\tilde{x}} \end{bmatrix}, \quad \boldsymbol{H}_{bm\tilde{x}} = \begin{bmatrix} H_{bmy} \\ H_{bmz} \end{bmatrix}, \quad (19)$$

$$\dot{\boldsymbol{W}}_m^{ref} = \boldsymbol{G}_m (\bar{\boldsymbol{p}}_{m\tilde{x}}^{d} - \bar{\boldsymbol{p}}_{m\tilde{x}}), \quad \bar{\boldsymbol{p}}_{m\tilde{x}}^{d} = \begin{bmatrix} \bar{p}_{my}^{d} \\ \bar{p}_{mz}^{d} \end{bmatrix}, \quad (20)$$

[4]Subscript "mcc" means momentum conservation control.

$\boldsymbol{J}_m(\boldsymbol{q}_m) \in \Re^{6\times9}$, $\boldsymbol{H}_{bm\tilde{x}}(\boldsymbol{q}_m) \in \Re^{2\times9}$ and $\boldsymbol{p}_{m\tilde{x}}(\boldsymbol{q}_m) \in \Re^2$ stand for the end-effector Jacobian, inertia coupling matrix and reduced the linear momentum w.r.t. the base coordinate frame. $(\circ)_{\tilde{x}}$ means that the respective x-axis element is ignored. $\boldsymbol{G}_m$ is a positive definite matrix, $\boldsymbol{D}_{mc}$ denotes a positive definite control damping matrix for the joints of the mini manipulator. We should note that $\bar{p}_{my}^{d}(t_{in})$ and $\bar{p}_{mz}^{d}(t_{in})$ are determined via sample-and-hold at t_{in}. Note that the null space vector $\boldsymbol{n}_{\boldsymbol{A}_{\tilde{x}}}$ can not be used around the singularity. Also, the acceleration of the end-tip of the macro manipulator is assumed to be sufficiently small, so that $\dot{\boldsymbol{V}}_M \approx \boldsymbol{0}$.

4.3 Other motion control strategies

To highlight the performance of the newly proposed momentum conservation strategy, we will employ comparative analysis with two other control strategies described in past studies on flexible-base robots: (i) vibration suppression plus reactionless end-effector path tracking [10]; (ii) end-effector path tracking plus vibration suppression in the null space of the manipulator Jacobian [11]. These two strategies are represented below to reflect the specifics of the proposed JEMRMS/SFA model.

First, with reference to (8), vibration suppression control for our model is arranged as:

$$\dot{\boldsymbol{W}}_m^{ref} = \boldsymbol{G}_M \dot{\boldsymbol{q}}_M, \quad (21)$$

where $\boldsymbol{G}_M \in \Re^{3\times3}$ denotes a positive definite matrix for additional (inertial) damping in the joints of the macro manipulator. Referring to (6) and (10), we can write:

$$\boldsymbol{G}_M \dot{\boldsymbol{q}}_M = \boldsymbol{H}_{Mm} \ddot{\boldsymbol{q}}_m + \dot{\boldsymbol{H}}_{Mm} \dot{\boldsymbol{q}}_m \quad (22)$$

and

$$\ddot{\boldsymbol{q}}_m^{ref} = \boldsymbol{H}_{Mm}^{+} (\boldsymbol{G}_M \dot{\boldsymbol{q}}_M - \dot{\boldsymbol{H}}_{Mm} \dot{\boldsymbol{q}}_m) + \boldsymbol{n}_{Mm}, \quad (23)$$

respectively. As described in [5], a vector from the *Reaction Null-Space* of JEMRMS/SFA can be derived as:

$$\boldsymbol{n}_{Mm} = (\boldsymbol{U} - \boldsymbol{H}_{Mm}^{+} \boldsymbol{H}_{Mm}) \boldsymbol{J}_m^{+} (\dot{\boldsymbol{V}}_e^{ref} - \dot{\boldsymbol{J}}_m \dot{\boldsymbol{q}}_m + \boldsymbol{J}_m \boldsymbol{H}_{Mm}^{+} \dot{\boldsymbol{H}}_{Mm} \dot{\boldsymbol{q}}_m), \quad (24)$$

where $\boldsymbol{U}$ denotes unit matrix. Finally, the control torque can be obtained by inserting (23) and (24) into the lower part of (17):

$$\boldsymbol{\tau}_{rmc} = \boldsymbol{H}_m \boldsymbol{H}_{Mm}^{+} (\boldsymbol{G}_M \dot{\boldsymbol{q}}_M - \dot{\boldsymbol{H}}_{Mm} \dot{\boldsymbol{q}}_m) + \boldsymbol{H}_m \boldsymbol{n}_{Mm} + (\boldsymbol{D}_m + \boldsymbol{D}_{mc}) \dot{\boldsymbol{q}}_m + \boldsymbol{c}_m, \quad (25)$$

where "*rmc*" means "reactionless motion control." Note that the approximation $\ddot{\boldsymbol{q}}_M \approx \boldsymbol{0}$ has been used since the joint acceleration of the macro part is considered as negligible.

The above equation satisfies two constraints, the *Reaction Null-Space* constraint $\boldsymbol{0} = \boldsymbol{H}_{Mm} \ddot{\boldsymbol{q}}_m + \dot{\boldsymbol{H}}_{Mm} \dot{\boldsymbol{q}}_m$ and

the end-effector constraint ${}^{\prime}\dot{\boldsymbol{V}}_e = \boldsymbol{J}_m\ddot{\boldsymbol{q}}_m + \dot{\boldsymbol{J}}_m\dot{\boldsymbol{q}}_m$. The algorithmic singularities are described by $\det \boldsymbol{A} = 0$, where $\boldsymbol{A} = [\boldsymbol{J}_m^T \; \boldsymbol{H}_{Mm}^T]^T$. It becomes then apparent that the above control law will restrict the manipulator motion in a quite conservative way.

Next, to alleviate the above problem, we decided to give up on reactionless motion control and to keep only vibration suppression control. Such strategy yields *almost* reactionless motion, provided the CoM does not accelerate/decelerate significantly. The respective control strategy ensures vibration suppression within the null space of the mini manipulator Jacobian:

$$\ddot{\boldsymbol{q}}_m^{ref} = \boldsymbol{J}_m^{+}({}^{\prime}\dot{\boldsymbol{V}}_e^{ref} - \dot{\boldsymbol{J}}_m\dot{\boldsymbol{q}}) + \boldsymbol{n}_{J_m}, \tag{26}$$

where

$$\boldsymbol{n}_{J_m} = (\boldsymbol{U} - \boldsymbol{J}_m^{+}\boldsymbol{J}_m)\boldsymbol{H}_{Mm}^{+} (\boldsymbol{G}_M\dot{\boldsymbol{q}}_M - \dot{\boldsymbol{H}}_{Mm}\dot{\boldsymbol{q}}_m + \boldsymbol{H}_{Mm}\boldsymbol{J}_m^{+}\dot{\boldsymbol{J}}_m\dot{\boldsymbol{q}}_m). \tag{27}$$

With this null space vector, two constraints are satisfied; the end-effector null space constraint $\boldsymbol{J}_m\ddot{\boldsymbol{q}}_m + \dot{\boldsymbol{J}}_m\dot{\boldsymbol{q}}_m = \boldsymbol{0}$ and the vibration suppression constraint (22). Hence, vibration suppression is achieved without disturbing the end-effector motion. The control torque is written as:

$$\boldsymbol{\tau}_{vsc} = \boldsymbol{H}_m\boldsymbol{J}_m^{+}({}^{\prime}\dot{\boldsymbol{V}}_e^{ref} - \dot{\boldsymbol{J}}_m\dot{\boldsymbol{q}}_m) + \boldsymbol{H}_m\boldsymbol{n}_{J_m} + (\boldsymbol{D}_m + \boldsymbol{D}_{mc})\dot{\boldsymbol{q}}_m + \boldsymbol{c}_m, \tag{28}$$

where "*vsc*" means "vibration suppression control."

5 Simulation Study

We use the MaTX simulation environment [12] and the respective SpaceDynX toolbox for modeling and control of space robots.

5.1 Initial conditions and simulations

Four simulations will be performed. The initial configurations for the macro and mini manipulators in all simulations are the same: $\boldsymbol{q}_M = [-10, 40, -110]^T$ deg and $\boldsymbol{q}_m = [20, 0, 0, 0, 50, -50, 0, 0, 45]^T$ deg, respectively. The desired end-effector path is a straight-line in the positive z direction. This allows for exciting the vibrations in the flexible joints 2 and 3. The orientation of the end-effector is to be kept constant during the motion. These settings can be also confirmed from Figure 3. The speed and acceleration along the straight-line path were calculated with the help of a fifth-order spline, with final time set to 20 s. The sampling time was set to 1 ms. The total time of the simulation — to 40 s. The gain matrices were chosen as follows:

$$\begin{aligned}
\boldsymbol{K}_M &= \text{diag}[8000, 8000, 8000]\ \text{Nm}^{-1},\\
\boldsymbol{D}_M &= \text{diag}[10, 10, 10]\ \text{Nsm}^{-1},\\
\boldsymbol{D}_m &= \text{diag}[10, 10, 10, 8, 8, 8, 8, 8, 8]\ \text{Nsm}^{-1},\\
\boldsymbol{D}_{mc} &= \text{diag}[1, 1, 1000, 1, 1, 1, 1, 1, 1]\ \text{Nsm}^{-1},\\
\boldsymbol{K}_d &= \text{diag}[10, 10, 10, 20, 20, 20]\ \text{s}^{-1},\\
\boldsymbol{K}_p &= \text{diag}[1000, 1000, 1000, 50, 50, 50]\ \text{s}^{-2},\\
\boldsymbol{G}_M &= \text{diag}[5000, 5000, 5000]\ \text{s}^{-1}.
\end{aligned}$$

As already explained the joint axes z_6 (z_b) and z_7 are parallel and only slightly displaced, which leads to excessive joint velocity. To alleviate the problem, the damping gain for the third joint of the mini manipulator was set to a high value.

In the first simulation (Sim. 1), reactionless motion control (25) was employed. In the second one (Sim. 2) — vibration suppression control (28) was used. In these two simulations, the distance from the initial configuration was set to 1.0 m, which was sufficient to reach an algorithmic singularity of reactionless motion. The third simulation (Sim. 3) was again with the same controller as Sim. 2, only the desired distance was set to 3.0 m in order to reach an algorithmic singularity of vibration suppression control. In the fourth simulation (Sim. 4), we utilized the momentum conservation control (18) to pass through the above algorithmic singularity of vibration suppression. The switching time t_{in} and t_{out} were set manually to 8 s and 15 s, respectively. The momentum feedback gain was set to $\boldsymbol{G}_m = \text{diag}[10, 10]\ \text{s}^{-1}$. The other settings were same as in Sim. 3.

5.2 Simulation results

The results from Sims. 1 and 2 are shown in Figure 4. In these figures, (a) and (b) display the joint deflection angles in the second and third joint of the macro arm, respectively, (c) shows the determinant $\det \boldsymbol{A}$, (d), (e) and (f) display the end-effector position along z and the respective position and orientation errors. Note that errors in the x and y directions (not shown) are of the same order of magnitude. The results from Sims. 3 and 4, on the other hand, are shown in Figure 5. Plots (a) to (e) have the same meaning as those in Figure 4. Figure 5 (f) displays the coupling linear momentum along the z-axis. In these figures, "position," "orientation" and "momentum" are abbreviated as "pos.," "ori." and "mom.," respectively.

From Figure 4 (c) it is apparent that the mini manipulator reaches an algorithmic singularity of reactionless motion around 10 s in Sim. 1. Motion cannot continue without destabilization beyond that point, hence the workspace of the end-effector is quite restricted (see Figure 4 (d)). In Sim. 2, on the other hand, it is seen that the end-effector can pass through the above singularity. From Figures 4 (a) and (b) it is seen that the flexible joints of the macro arm deflect somewhat in Sim. 2, however the magnitude is not so significant, so we conclude that *almost* reactionless motion is achieved. From Figures 4 (e)

and (f), it is, also, seen that the amplitudes of the positioning/orientation error of the mini manipulator are quite small in Sim. 2.

On the other hand, from Figures 5 (c) and (d) it can be seen that an algorithmic singularity of vibration suppression control is reached in Sim. 3, around 15 s. In addition, from Figure 5 (a) and (b), it can be observed that the joint deflections of the macro manipulator have increased when compared to those in Figure 4. This result is not unexpected since a faster motion implies a larger CoM acceleration of the mini manipulator, and hence larger disturbances in the flexible joints.

Finally, from Sim. 4 it is seen that the end-effector can move through the above singularity under linear momentum conservation control. Figure 5 (f) shows that the CoM velocity stays nearly constant from 8 s to 15 s in Sim. 4. With this strategy, a suitable CoM velocity can be realized such that the end-effector can travel larger distances without the need to escape singularities.

6 Conclusions

We have proposed a new control method for end-effector path tracking with simultaneous vibration suppression on a flexible-base robot, in the presence of algorithmic singularities of vibration suppression. The idea is quite simple: move through the singularity by switching to momentum conservation control during the motion, i.e. by conserving the nonzero momentum upon entering a respecified neighborhood of the singularity. When leaving the neighborhood, switch back to vibration suppression control. We have shown how to implement the controller with JEMRMS/SFA. The simulation results have demonstrated that with this controller it is possible to obtain stable and *almost* reactionless motion while tracking a straight-line path within a large portion of workspace, while other methods failed to accomplish this task.

Further analysis and a more detailed study will be needed, though, to determine the limits of the proposed method, including its task-dependency, robustness and sensitivity to modeling errors.

References

[1] A. Sharon and D. Hardt, "Enhancement of Robot Accuracy using End-Point Feedback and a Macro-Micro Manipulator System," in Proc. ACC, San Diego, CA, 1984, pp. 1836–1842.

[2] M. W. Spong, "Modeling and Control of Elastic Joint Robotics," *in Trans. of the ASME: Journal of Dynamic System, Measurement, and control*, 1987, vol. 31, No. 4, pp. 310–319.

[3] K. Yoshida, D. N. Nenchev and M. Uchiyama, "Vibration Suppression and Zero Reaction Maneuvers of Flexible Space Structure Mounted Manipulators," *Journal of Smart Materials and Structures*, IOP Publishing Ltd., Bristol, UK, 1999, vol. 8, no. 6, pp. 847–856.

[4] S. Abiko and K. Yoshida, "An Adaptive Control of a Space Manipulator for Vibration Suppression," *in Proc. IEEE/RSJ Int. Conf. Intell. Robot. Syst.*, Edmonton, Canada, Aug. 2005, pp. 2888–2893.

[5] Y. Fukazu *et. al*, "Reactionless Resolved Acceleration Control with Vibration Suppression Capability for JEMRMS/SFA," *Robotics and Biomimetics*, Bangkok, Thailand, Feb. 2009, pp. 1359–1364.

[6] S. H. Lee and W. J. Book, "Robot Vibration Control using Inertial Damping Forces," in *Proc. 8th CISM.–IFToMM Symp. RoManSy 8*, Cracow, Poland, Jul. 1990, pp. 252–259.

[7] D. N. Nenchev *et. al*, "Reaction Null-Space Control of Flexible Structure Mounted Manipulator Systems," *IEEE Trans. on Robotics and Automation*, Dec. 1999, vol. 15, no. 6, pp. 1011–1023.

[8] N. Hara *et. al*, "Singularity-Consistent Torque Control of a Redundant Flexible-Base Manipulator," in *Motion and Vibration Control: Selected Papers from MOVIC 2008*, H. Ulbrich and L. Ginzinger, Eds. Dordrecht, Netherlands: Springer Netherlands, Dec. 2008, pp. 103–112.

[9] Y. Wakabayashi *et. al*, "Performance of Japanese Robotic Arms of the International Space Station," *IEEE Trans. Robot. Automat.*, 1999, vol. 15, no. 6, pp. 1011–1023.

[10] T. Hishinuma and D. N. Nenchev, "Singularity-Consistent Vibration Suppression Control with a Redundant Manipulator Mounted on a Flexible Base," in *Proc. 2006 IEEE/RSJ Int. Conf. on Intelligent Robots and Systems*, Beijing, China, Oct. 9–15, 2006, pp. 3237–3242.

[11] Y. Fukazu *et. al*, "Pseudoinverse-based motion control of a redundant manipulator on a flexible base with vibration suppression," *J. of Robotics and Mechatoronics*, 2008, vol. 20, no. 4, pp. 621–627.

[12] M. Koga and K. Furuta, "MaTX: A High-Performance Programming Language (Interpreter and Compiler) for Scientific and Engineering Computation," in *IEEE Symposium on Computer-Aided Control System Design*, Napa, California, Mar. 1992, pp. 15–22.

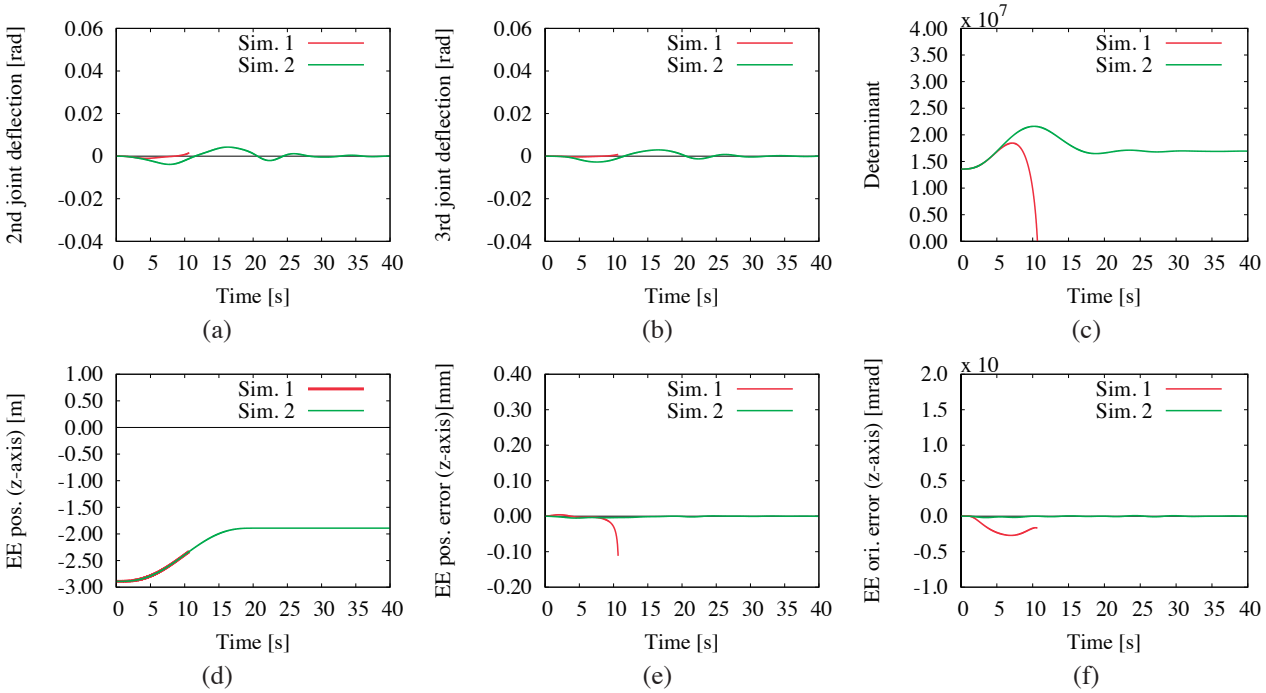

Figure 4. Reactionless motion control (Sim. 1) vs vibration suppression control (Sim. 2). With vibration suppression control it is possible to go through the algorithmic singularity of reactionless motion control.

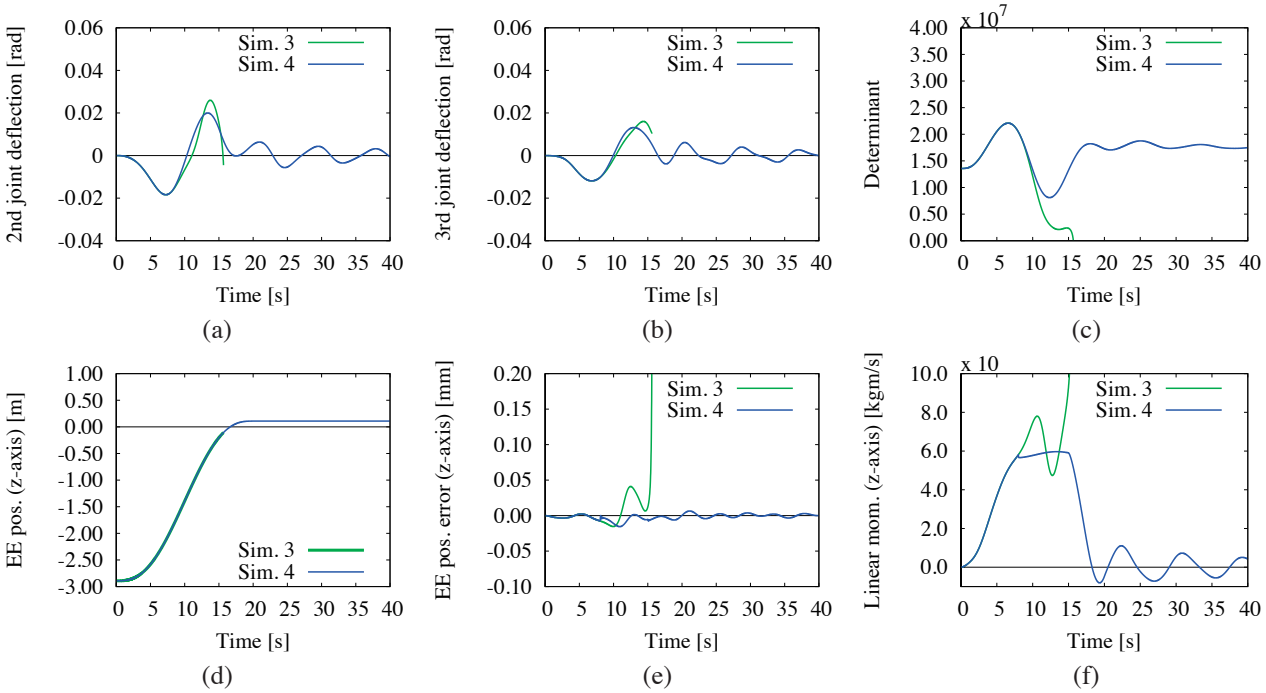

Figure 5. Vibration suppression control (Sim. 3) vs momentum conservation control (Sim. 4). With momentum conservation control it is possible to go through the algorithmic singularity of vibration suppression control.